Fast Characterization of Functionalized Silica Materials by Silicon-29 Surface-Enhanced NMR Spectroscopy Using Dynamic Nuclear Polarization

Moreno Lelli,[†] David Gajan,[‡,||] Anne Lesage,[†] Marc A. Caporini,[§] Veronika Vitzthum,[§] Pascal Miéville,[§] Florent Héroguel,[‡,||] Fernando Rascón,[‡,||] Arthur Roussey,[‡] Chloé Thieuleux,[‡] Malika Boualleg,[‡] Laurent Veyre,[‡] Geoffrey Bodenhausen,[§,¶,⊥] Christophe Copéret,[‡,||] and Lyndon Emsley*,[†]

[†]Centre de RMN à Très Hauts Champs, Université de Lyon (CNRS/ENS Lyon/UCB Lyon 1), 69100 Villeurbanne, France

[‡]Institut de Chimie de Lyon, C2P2, UMR 5265, Université de Lyon (CNRS−Université Lyon 1−ESCPE Lyon), ESCPE Lyon, 69100 Villeurbanne, France

[§]Institut des Sciences et Ingénierie Chimiques, Ecole Polytechnique Fédérale de Lausanne (EPFL), 1015 Lausanne, Switzerland

[||]Department of Chemistry, ETH Zürich, CH-8093 Zürich, Switzerland

[¶]Département de Chimie, Ecole Normale Supérieure, 75231 Paris Cedex 05, France

[⊥]CNRS, UMR 7203, and Université de Pierre-et-Marie Curie, 75005 Paris, France

Ⓢ *Supporting Information*

ABSTRACT: We demonstrate fast characterization of the distribution of surface bonding modes and interactions in a series of functionalized materials via surface-enhanced nuclear magnetic resonance spectroscopy using dynamic nuclear polarization (DNP). Surface-enhanced silicon-29 DNP NMR spectra were obtained by using incipient wetness impregnation of the sample with a solution containing a polarizing radical (TOTAPOL). We identify and compare the bonding topology of functional groups in materials obtained via a sol−gel process and in materials prepared by post-grafting reactions. Furthermore, the remarkable gain in time provided by surface-enhanced silicon-29 DNP NMR spectroscopy (typically on the order of a factor 400) allows the facile acquisition of two-dimensional correlation spectra.

Hybrid organic−silica materials are an important class of composite materials of widespread interest in modern chemistry, ranging from fundamental developments to advanced applications. They consist of organic parts which are covalently bound to a silica matrix.[1] Their preparation involves either post-grafting of organosilicon reagents, typically organotrialkoxysilane, onto silica supports or direct co-hydrolysis and co-condensation of organotrialkoxysilane with tetraalkoxysilane precursors in sol−gel processes with[2−5] or without[6−8] structure-directing agents. When structure-directing agents are used, it is also possible to control the organization of the materials (e.g., cubic, vermicular, or hexagonal networks) and the density and placement of the organic functionalities (regular distributions on the surface of the pores and/or in the walls of the materials), providing access to highly tunable materials and thereby to numerous properties.

Understanding the activity of functionalized silica materials requires a molecular-level characterization of the functional groups, particularly their conformations and modes of binding/interaction to/with the surface. In particular, it is well recognized that a given surface silicon atom bearing a functional group can have a variable number n of Si−O−Si bonds, leading to so-called T_1, T_2, or T_3 substructures. These bonding schemes lead to very different geometries on the surface, as illustrated in Figure 1A for organic−inorganic hybrid materials containing phenol functionalities.[9] Knowledge of the surface incorporation patterns and the conformations of functional groups for such materials is clearly an essential step toward developing smart functional substrates.

There are no readily available analytical methods to characterize different surface incorporation patterns and conformations. Diffraction techniques are not well suited for structural studies of surface species, and infrared spectroscopy does not provide enough information for such complex organic functionalities. Nuclear magnetic resonance studies of silica-based materials are thus particularly attractive. Cross-polarization magic angle spinning (CPMAS) ^{29}Si NMR studies have been extensively used where applicable, since they provide narrow spectra with atomic resolution that can easily characterize the bonding environment of silicon atoms near the surface.[4,8,10−19] However, NMR suffers from low sensitivity, and in many cases the functionalized silicon T_n sites are too dilute to be readily observed; the spectra provide mainly information about the bulk surface species Q_4 and proton-rich Q_n sites (Si−OH). In most cases, little or no evidence of incorporation patterns of the functional groups can be obtained because of the low sensitivity of the method, unless one resorts to very long, often unreasonable, acquisition times. Further, as a direct result of this low sensitivity, multidimensional NMR methods to characterize the conformations of the functional groups are precluded.

In recent work[9] we overcame the sensitivity problem of the NMR technique for surfaces by combining magic angle spinning (MAS) with dynamic nuclear polarization (DNP).[20,21] We adapted methods developed for studying biomolecular solids[21] to functionalized silica materials by dissolving the biradical TOTAPOL[22] into a suitable solvent mixture, which was then used to wet the solid by incipient wetness impregnation. At low
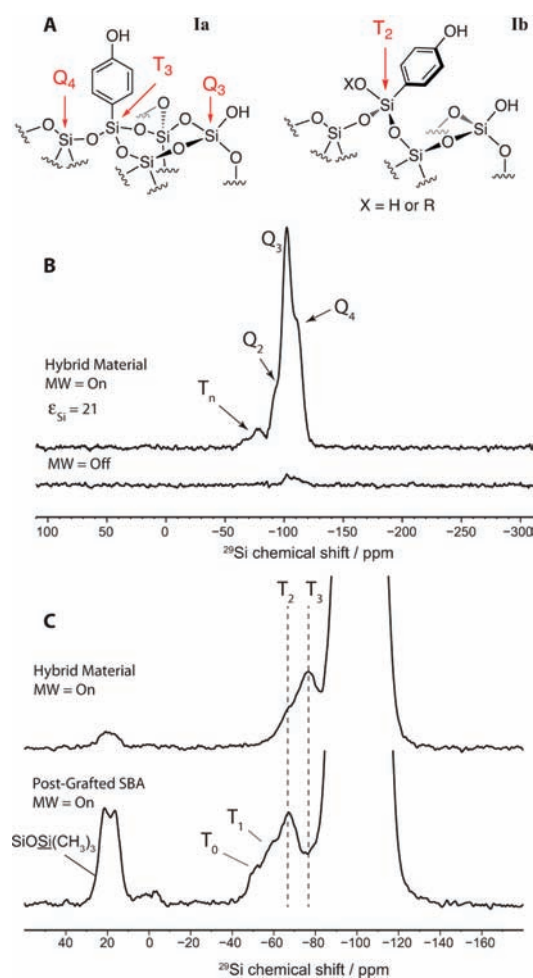
Figure 1. (A) Structures of the T_3 (**Ia**) and T_2 species (**Ib**) that are present on phenol-functionalized silica surfaces. (B) Silicon-29 CPMAS spectra of **I** with (upper) and without (lower) microwave irradiation at 263 GHz to induce DNP (9.4 T, 400.1 and 79.5 MHz ^{1}H and ^{29}Si Larmor frequencies, respectively). Both spectra were recorded at sample temperatures of ∼105 K using 2048 scans, with a polarization build-up interval between scans of 1 s and a sample spinning frequency $\omega_{rot}/2\pi =$ 8 kHz. (C) Silicon-29 CP MAS spectra of two different phenol-functionalized mesoporous materials: hybrid material (upper, 10 240 scans, 2.8 h) for which the organic phenol moiety has been directly incorporated onto the silica framework by a sol−gel process, and mesoporous material obtained by post-grafting the phenolic units onto an SBA-15 matrix (lower, 26 624 scans, 7.4 h). All samples were wetted with 9.2 mM TOTAPOL in 90:10 D_2O/H_2O. The signals around 20 ppm correspond to surface $SiMe_3$ groups.

temperatures (∼100 K) we showed that it is possible to transfer magnetization upon saturation of the highly polarized electron spin to the ^{1}H nuclei of the sample by continuous irradiation of the electron resonance with intense microwaves generated by a gyrotron.[23] We were able to transfer the enhanced ^{1}H magnetization by cross-polarization (CP) to the carbon-13 nuclei of the organic functional groups attached to a silica surface. In this way, it was possible to enhance the sensitivity of the surface-anchored organic species by a factor $\varepsilon_C = 20-50$ compared to a similar experiment without DNP. This made it possible to acquire surface-enhanced ^{13}C spectra and 2D ^{1}H−^{13}C correlation experiments of highly dilute systems at natural abundance (0.2 mmol of the organic functional group per gram of sample) in a few minutes.[9]

Here we show that surface-enhanced NMR spectroscopy using DNP can be extended to silicon-29 nuclei on surfaces, allowing rapid acquisition of multidimensional spectra. We determine the incorporation patterns and conformations of functional groups in a range of hybrid materials. Figure 1B shows the dramatic effect on the sensitivity of the ^{29}Si CPMAS spectrum of compound **I** (all the materials used here were prepared as described in the Supporting Information). The figure shows spectra recorded with and without microwave irradiation of materials impregnated with 9.2 mM TO-TAPOL in a 90:10 D_2O:H_2O solution added to a dry powder of mesostructured hybrid material. In the ordinary low-temperature spectrum, acquired in 35 min with 2048 scans, only a few Q_n sites are (barely) observable. Note that CP from ^{1}H to ^{29}Si preferentially "lights up" the surface Q_n sites of the material, since there are no ^{1}H atoms in the bulk. The Q_n sites are actually of little interest in this study. We focus attention on the distribution of the surface T_n sites, which indicates the incorporation of organic functionalities, with resonances between −50 and −80 ppm. From the synthetic method, we expect a ratio of around 1 silicon atom linked to a functional group per 30 silicon atoms (either surface or bulk) (see Supporting Information). Since there are far fewer T_n than Q_n sites, the former are invisible in the spectrum of Figure 1B without DNP. In spectacular contrast, the spectrum obtained with DNP with the same number of scans in the same time is enhanced by a factor $\varepsilon_{Si} \approx 21$, and both the Q_n and T_n sites are now clearly visible, allowing their detailed characterization.

Figure 1C shows a comparison of DNP NMR spectra of material **I** prepared by two different methods, either by the sol−gel process or by post-grafting the phenol group onto a SBA-15-type support (see Supporting Information for details). The spectra clearly show very different patterns for the functionalized T_n species, where the silicon atoms are directly bound to at least one organic moiety. The figure indicates the characteristic resonance frequencies at −77 ppm for T_3 species $(SiO)_3SiR$ and at −66 ppm for the T_2 forms ($(SiO)_2 SiR(OX)$, X = H or Et) and upfield bands (−60 ppm) related to T_1 ($(SiO)SiR(OX)_2$), as well as a trace amount of physisorbed organosilicon compound, $(XO)_3SiR$ (T_0, −57 ppm). From the spectra of Figure 1C, it is immediately apparent that grafting $(R'O)_3SiR$ groups onto SBA-15 produces a wider distribution of T_n species, centered on T_2, as compared to the hybrid method which produces mainly T_3 surface sites, with a few T_2 sites. The hybrid material is clearly a better substrate for controlled chemistry.

We note that the intensities in the spectra allow qualitative estimates of the relative populations of the different Q_n and T_n sites. As with any CPMAS experiment, the ^{1}H−^{29}Si CP transfer used to enhance the surface depends to some extent on the local proton density. For example, in material **I**, the Q_n sites can be polarized from the protons of the SiOH groups that are only two bonds away, while for the T_n sites the ^{1}H spins are three bonds away, in the ortho positions on the aromatic ring. This situation can be contrasted with the case of SBA-15 functionalized with SiH groups (**II**, Figure 2A), where the ^{1}H spin is directly linked to the T_n site. Indeed we see in Figure 2B that, at very short CP mixing times (τ_{CP} = 0.5 ms), the T_n sites are selectively enhanced, with almost no signal from Q_n sites. The signals of the Q_n sites build up progressively as τ_{CP} is increased and polarization is transferred from more distant spins. This suggests that the enhanced polarization diffuses from the radical across the entire dipolar-coupled proton network, including the surface protons, consistent with observations of DNP in biosolids.[24,25] Direct ^{1}H-to-^{29}Si transfer by CP from solvent protons farther away from the

2105

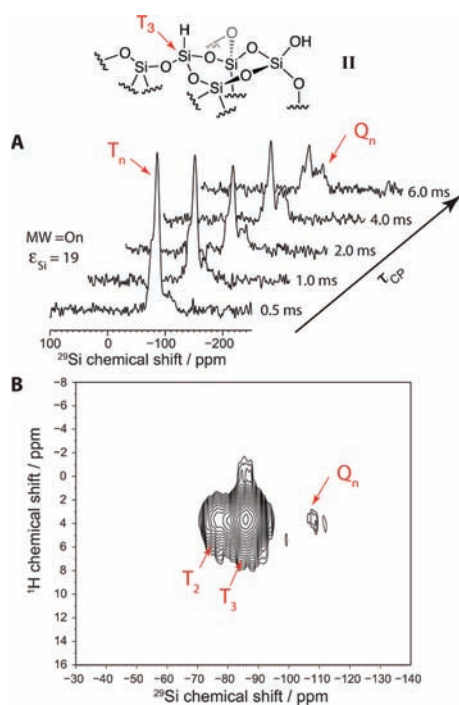dx.doi.org/10.1021/ja110791d |*J. Am. Chem. Soc.* 2011, 133, 2104–2107

Figure 2. (A) DNP-enhanced silicon-29 CPMAS spectra of **II** as a function of the CP mixing time τ_{CP}. Spectra were recorded with 16 scans. (B) Contour plot of a two-dimensional $^1H-^{29}Si$ spectrum of **II** recorded with DNP. 64 t_1 increments with eight scans each were recorded with τ_{CP} = 1.0 ms. Total experimental time was 8.5 min.

Figure 3. DNP-enhanced silicon-29 CPMAS spectra of a series of functionalized mesoporous hybrid materials. The organic fragments incorporated into the silica matrix are indicated. Spectra were recorded with 2048 scans in a total experimental time of 35 min each, with τ_{CP} = 6.0 ms. The dilution factors among functionalized and nonfunctionalized silicon atoms used in the synthesis of these hybrid materials were 1/30 for **III** and **IV** and 1/19 for **V** and **VI** (see Supporting Information).

surface (if present) is clearly much less efficient. In the spectra of Figure 2B, the surface SiH groups were observed with an enhancement of ε_{Si} = 19 and with only 16 scans in 24 s! Under such enhanced conditions, we can acquire 2D $^1H-^{29}Si$ correlation spectra of the surface species in only 8 min. The 2D spectrum of Figure 2C shows that both T_2 and T_3 silicon sites correlate with the SiH protons.

To further explore the conformation of the functional groups and to test the generality of the approach, we acquired surface-enhanced ^{29}Si spectra from a range of materials. Notably, DNP yielded high-sensitivity spectra with ε_{Si} = 29 for pure nonporous flame silica (surface area of 200 m^2/g) impregnated with the $H_2O/D_2O/$TOTAPOL solution (see Supporting Information). Evidently, the porous nature of the silica material is *not* crucial for a surface DNP enhancement.

In Figure 3 we show spectra obtained with surface-enhanced DNP applied to different functionalized hybrid materials (**III**−**VI**). In all cases the DNP enhancement factors are good ($\varepsilon_{Si} \approx 20$, one case $\varepsilon_{Si} \approx 10$), and in all these materials T_3 along with T_2 species are clearly observed. For materials **V** and **VI**, the T_3 species occur with a characteristic chemical shift of −66 ppm (instead of −77 ppm as in the phenol derivatives) since the silicon atoms are bound to an aliphatic −CH$_2$− moiety instead of an aromatic unit. The shorter distance between the aliphatic CH$_2$ protons and T_3 silicon atom in compounds **V** and **VI** compared to **III** and **IV** explains the more efficient CP transfer, and thus the more intense T_3 signals. As with the hybrid form of **I**, incorporation of the functional groups through surface T_3 sites is highly favored in all these materials.

The facile acquisition of 2D $^1H-^{29}Si$ correlation spectra allows us a more detailed conformational analysis of the functional groups. In particular, Figure 4 shows spectra of materials **V** and
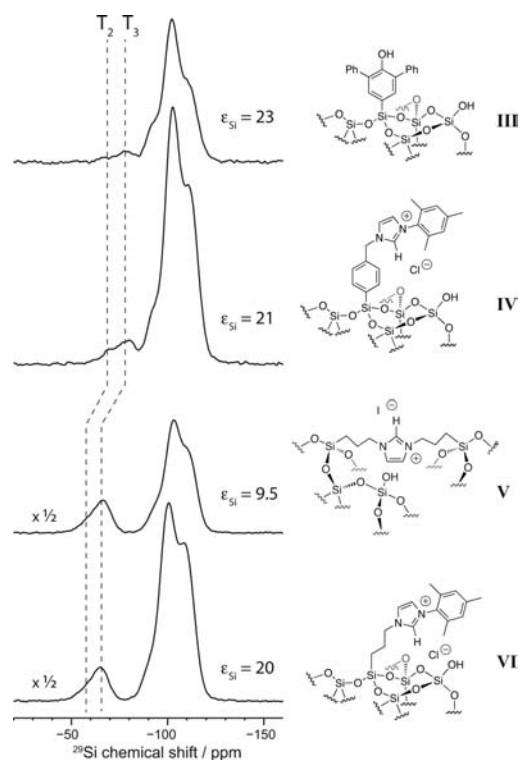
VI. The short mixing time (τ_{CP} = 0.5 ms) favors transfer from ^1H in close proximity to silicon atoms. As expected, it is apparent that the T_3 nuclei correlate with the aliphatic protons of the organic −CH$_2$− moiety. In contrast, the Q_3 and Q_4 silica sites correlate with the SiOH protons at 4−5 ppm (and possibly with protons of the frozen solvent) and, remarkably, with the aromatic imidazolium unit (at ∼9 ppm). This indicates a close proximity between the imidazolium units and the silica framework. This observation is in line with expectations for compound **V** (Figure 4A), since it is anchored to the silica surface at two points and is thus embedded in the solid.

Noteworthy, when the same experiment is performed on compound **VI**, which contains a flexible tether (propyl chain) with only one anchor at the surface, the spectrum of Figure 4B shows that we observe a strong correlation peak between the silica surface Q_3 sites and both the imidazolium and the mesitylene protons (not resolved in the proton dimension) of the organic unit. In this case the aromatic groups might be expected to point outward into the cavity. However, the two-dimensional correlation spectrum clearly shows a close proximity between the aromatic rings and the Q_n sites of the surface, suggesting that the imidazolium units (or at least a significant fraction of them) are likely to be folded back toward the silica surface, rather than being in the cavity. Thus, this scaffold should be used with care as a support for active sites.

Imidazolium moieties have an affinity for polar media like water,[26] so it is surprising that these grafted species do not "stand up" but are flattened out on the surface. Apparently, with a flexible tether, electrostatic interactions can dominate over
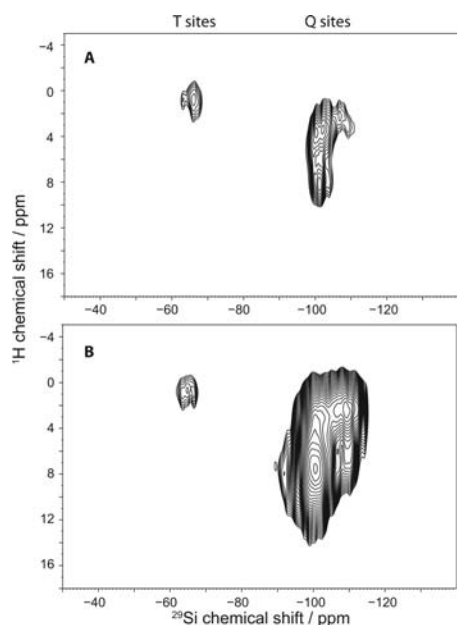
Figure 4. Contour plots of a surface-enhanced two-dimensional $^1H-^{29}Si$ correlation spectrum of **V** (A) and **VI** (B). For each spectrum a total of 48 t_1 increments with 112 scans each were recorded in a total experimental time of 1.5 h each, with τ_{CP} = 0.5 ms.

solvation effects. Note that while these spectra thus clearly contain conformational information, more detailed interpretation would require a quantitative study and the investigation of a wider range of organic functionalities. Note also that no method other than NMR can determine such conformational features.

In conclusion, DNP-enhanced ^{29}Si spectra allow us to determine the incorporation patterns of functional groups on silica surfaces in a few minutes and confirm that a controlled sol−gel process favors incorporation of functional groups through T_3 sites, while postgrafting leads to more disordered surface attachment.

Furthermore, two-dimensional $^1H-^{29}Si$ correlation spectra with good signal-to-noise ratios can be obtained (hours rather than months), which was previously inconceivable for this kind of material using standard NMR technology. Further improvement can be envisaged since other state-of-the-art NMR techniques, such as proton detection or Carr−Purcell−Meiboom−Gill (CPMG),[11] may also benefit from DNP enhancement. The spectra acquired here clearly show that functional groups with flexible chains do not necessarily point into the pore cavities but can be at least in part folded back onto the surface. This will have consequences regarding the orientation, mobility, and activity of materials based on these species. These results clearly demonstrate the power of multidimensional ^{29}Si surface-enhanced NMR spectroscopy using DNP, which is likely to become a routine method of characterization. Multi-dimensional ^{29}Si DNP provides a simple and general approach to the characterization of surfaces with atomic resolution.

■ ASSOCIATED CONTENT

ⓈSupporting Information. Sample preparation and experimental methods. This material is available free of charge via the Internet at http://pubs.acs.org.

■ AUTHOR INFORMATION

Corresponding Author
lyndon.emsley@ens-lyon.fr

■ REFERENCES

(1) Hüsing, N.; Schubert, U. In *Functional Hybrid Materials*; Gómez-Romero, P.Sanchez, C., Eds.; Wiley: Weinheim, 2004; pp 86−121.
(2) Inagaki, S.; Guan, S.; Fukushima, Y.; Ohsuna, T.; Terasaki, O. *J. Am. Chem. Soc.* **1999**, *121*, 9611−9614.
(3) Melde, B. J.; Holland, B. T.; Blanford, C. F.; Stein, A. *Chem. Mater.* **1999**, *11*, 3302−3308.
(4) Asefa, T.; MacLachlan, M. J.; Coombs, N.; Ozin, G. A. *Nature* **1999**, *402*, 867−871.
(5) Hoffmann, F.; Cornelius, M.; Morell, J.; Fröba, M. *Angew. Chem., Int. Ed.* **2006**, *45*, 3216−3251.
(6) Boury, B.; Corriu, R. J. P. *Chem. Commun.* **2002**, 795−802.
(7) Brinker, J.; Scherer, G. W. *Sol-Gel Science: The Physics and Chemistry of Sol-Gel Processing*; Academic Press: San Diego, CA, 1990.
(8) Athens, G. L.; Shayib, R. M.; Chmelka, B. F. *Curr. Opin. Colloid Interface Sci.* **2009**, *14*, 281−292.
(9) Lesage, A.; Lelli, M.; Gajan, D.; Caporini, M. A.; Vitzthum, V.; Miéville, P.; Alauzun, J.; Roussey, A.; Thieuleux, C.; Mehdi, A.; Bodenhausen, G.; Copéret, C.; Emsley, L. *J. Am. Chem. Soc.* **2010**, *132*, 15459−15461.
(10) Mao, K.; Pruski, M. *J. Magn. Reson.* **2010**, *203*, 144−149.
(11) Mao, K.; Kobayashi, T.; Wiench, J. W.; Chen, H. T.; Tsai, C. H.; Lin, V. S. Y.; Pruski, M. *J. Am. Chem. Soc.* **2010**, *132*, 12452−12457.
(12) Rawal, A.; Smith, B. J.; Athens, G. L.; Edwards, C. L.; Roberts, L.; Gupta, V.; Chmelka, B. F. *J. Am. Chem. Soc.* **2010**, *132*, 7321−7337.
(13) Bracco, S.; Comotti, A.; Valsesia, P.; Chmelka, B. F.; Sozzani, P. *Chem. Commun.* **2008**, 4798−4800.
(14) Brouwer, D. H.; Kristiansen, P. E.; Fyfe, C. A.; Levitt, M. H. *J. Am. Chem. Soc.* **2005**, *127*, 542−543.
(15) Cadars, S.; Mifsud, N.; Lesage, A.; Epping, J. D.; Hedin, N.; Chmelka, B. F.; Emsley, L. *J. Phys. Chem. C* **2008**, *112*, 9145−9154.
(16) Dogan, F.; Hammond, K. D.; Tompsett, G. A.; Huo, H.; Conner, W. C.; Auerbach, S. M.; Grey, C. P. *J. Am. Chem. Soc.* **2009**, *131*, 11062−11079.
(17) Fyfe, C. A.; Brouwer, D. H.; Lewis, A. R.; Villaescusa, L. A.; Morris, R. E. *J. Am. Chem. Soc.* **2002**, *124*, 7770−7778.
(18) Hedin, N.; Graf, R.; Christiansen, S. C.; Gervais, C.; Hayward, R. C.; Eckert, J.; Chmelka, B. F. *J. Am. Chem. Soc.* **2004**, *126*, 9425−9432.
(19) Liu, C. Q.; Lambert, J. B.; Fu, L. *J. Am. Chem. Soc.* **2003**, *125*, 6452−6461.
(20) Becerra, L. R.; Gerfen, G. J.; Temkin, R. J.; Singel, D. J.; Griffin, R. G. *Phys. Rev. Lett.* **1993**, *71*, 3561−3564.
(21) Hall, D. A.; Maus, D. C.; Gerfen, G. J.; Inati, S. J.; Becerra, L. R.; Dahlquist, F. W.; Griffin, R. G. *Science* **1997**, *276*, 930−932.
(22) Song, C. S.; Hu, K. N.; Joo, C. G.; Swager, T. M.; Griffin, R. G. *J. Am. Chem. Soc.* **2006**, *128*, 11385−11390.
(23) Rosay, M.; Tometich, L.; Pawsey, S.; Bader, R.; Schauwecker, R.; Blank, M.; Borchard, P. M.; Cauffman, S. R.; Felch, K. L.; Weber, R. T.; Temkin, R. J.; Griffin, R. G.; Maas, W. E. *Phys. Chem. Chem. Phys.* **2010**, *12*, 5850−5860.
(24) Barnes, A. B.; De Paepe, G.; van der Wel, P. C. A.; Hu, K. N.; Joo, C. G.; Bajaj, V. S.; Mak-Jurkauskas, M. L.; Sirigiri, J. R.; Herzfeld, J.; Temkin, R. J.; Griffin, R. G. *Appl. Magn. Reson.* **2008**, *34*, 237−263.
(25) van der Wel, P. C. A.; Hu, K. N.; Lewandowski, J.; Griffin, R. G. *J. Am. Chem. Soc.* **2006**, *128*, 10840−10846.
(26) Padua, A. A. H.; Gomes, M. F.; Lopes, J. N. A. C. *Acc. Chem. Res.* **2007**, *40*, 1087−1096.